AN ADVANCED STUDY OF SILICON PHOTOMULTIPLIER

P. Buzhan, B. Dolgoshein*, A. Ilyin, V. Kantserov, V. Kaplin, A. Karakash, A. Pleshko, E. Popova, S. Smirnov, Yu. Volkov

Moscow Engineering and Physics Institute, Moscow, Russia

L. Filatov and S. Klemin

"Pulsar" Enterprise, Moscow, Russia

F. Kayumov

Lebedev Physical Institute, Moscow, Russia

ABSTRACT

An advanced study of new photo detector - Silicon Photomultiplier (SiPM) is presented. SiPM consists of many ($\sim 10^3$ mm^{-2}) silicon micro pixels, which are independent photon micro-counters working in limited Geiger mode with a gain of 10^6. The SiPM output signal is a sum of the signals from a number of pixels fired by photons. The main features of SiPM are: low excess noise factor, the photon detection efficiency at the level of vacuum PMT, low bias voltage ($\sim$24V). The timing of the SiPM is about 30 ps for 10 photoelectrons. The possibilities of SiPM applications based on experimental tests are demonstrated: sci fiber readout, scintillator-shifter system readout, and possible application for hadron calorimeters.

*Corresponding author. E-mail address: boris@mail.cern.ch

1 Introduction

The Silicon Photomultiplier (SiPM) is a multipixel semiconductor photodiode, where the pixels are joint together on common silicon substrate[1]. Each SiPM pixel operates in limited Geiger mode, under bias voltage of 10-20% more than breakdown voltage, so each carrier generated by photons or thermally gives rise to a Geiger-type discharge. This Geiger discharge is stopped when the voltage goes down below breakdown value due to external resistor R on each pixel (typical R value is about 100-200 kΩ). This resistor also serves as a decoupling element between the individual pixels because $C_{pixel} \cdot R_{pixel} \sim 10^{-8}s \gg t_{discharge}$, where discharge time $t_{discharge} < 1$ ns.

Actually, each SiPM pixel operates as an independent photon Geiger micro-counter (like a single pixel device - single photon avalanche diode SPAD[2]), and the pixel Geiger signal does not depend on a triggered carrier number, which fires the pixel ("Geiger mode"). Single pixel gain is determined by the charge accumulated in pixel capacity C_{pixel}: $Q_{pixel} = C_{pixel} \cdot (V_{bias} - V_{breakdown})$. Typically, $C_{pixel} \simeq$100 fF, and V_{bias}-$V_{breakdown} \simeq$ a few volts, so $Q_{pixel} \simeq$ few times 100 pC and the single pixel "gain" is about 10^6, i.e., the same order as vacuum PMT gain. The pixel size is of 15 to 70 μm, and the total number of SiPM pixels is 100-4000 mm^{-2}. Because all SiPM pixels work together on common load, the output signal is a sum of the signals from all pixels fired. So such a number of pixels, where each element operates digitally as a binary device, works as an analogue detector, which can measure light intensity.

2 SiPM Description and Performance

2.1 SiPM topology

Figure 1a shows, as an example, the microphotograph of SiPM with pixel size 42x42 μm^2, and a total pixel number m=576 on the area of 1 mm^2. The SiPM topology is shown in Fig. 1b. A few micron epitaxy layer on low resistive p substrate forms the drift region with low built-in electric field (see Fig. 1c). The thin depletion region (0.7-0.8 μm) between the p$^+$ and n$^+$ layers with very high electric field (3 - 5)$\cdot 10^5$ V/cm is created, where the conditions for Geiger mode discharge take place ($V_{bias} > V_{breakdown}$). The electrical decoupling between the adjacent pixels is provided by polysilicon resistive strips and uniformity of the electric field within a pixel by the n$^-$ guard rings around each pixel (Fig. 1a,b). All 576 pixels are connected by common Al strips, in order to readout the SiPM signal.

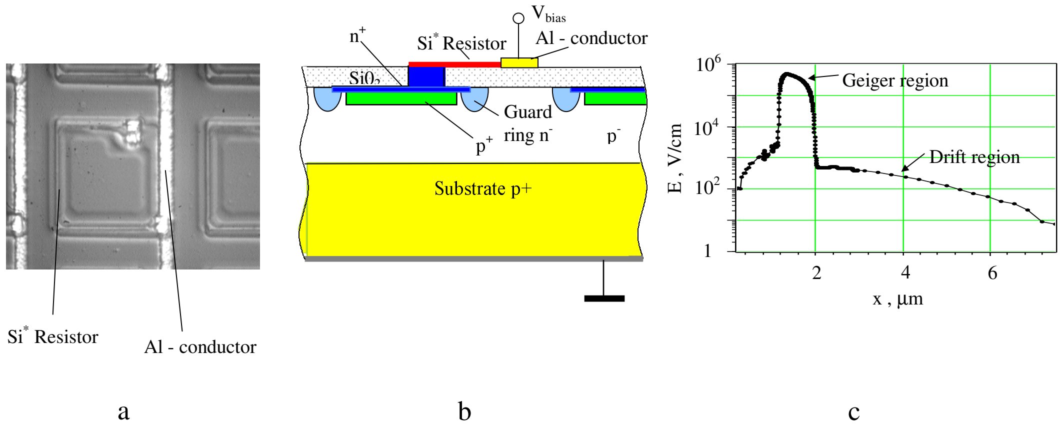

Figure 1: (a) Silicon photomultiplier microphotograph, (b) topology and (c) electric field distribution in epitaxy layer.

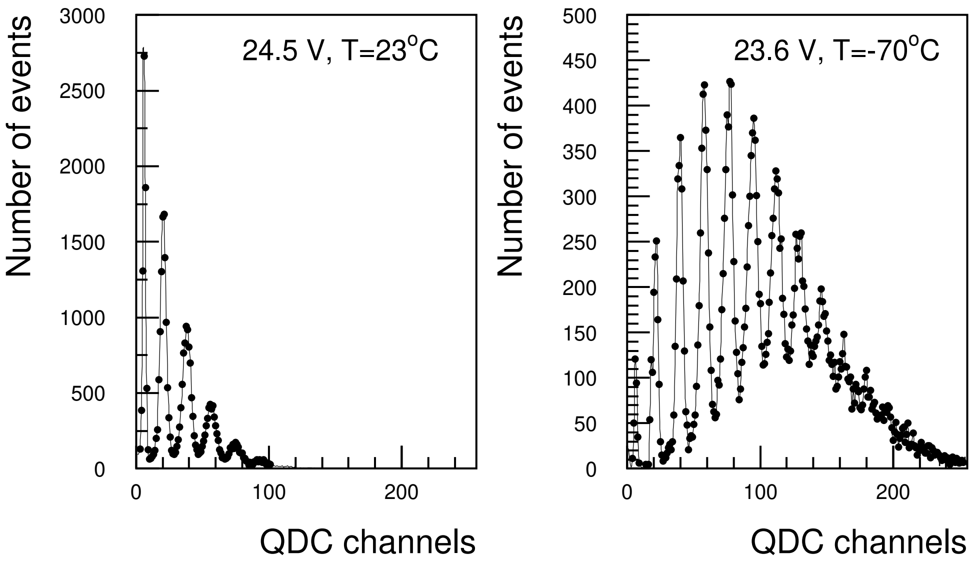

Figure 2: SiPM pulse height spectra.

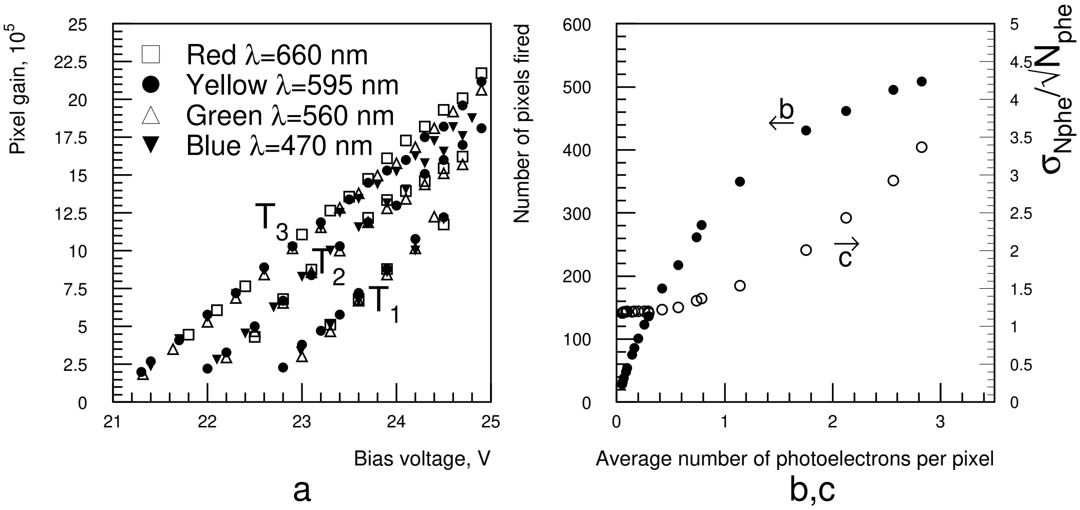

Figure 3: SiPM single pixel gain (a) for different temperatures: T_1=+22^{o}C, T_2=-22^{o}C, T_3=-61^{o}C; (b) SiPM signal saturation for m=576, and (c) signal dispersion.

2.2 SiPM Pulse Height Spectrum

The SiPM pulse height spectra from a low-intensity light emission diode (LED) source are shown in Fig. 2, for two temperatures 23^{o}C and -70^{o}C. We can conclude from Fig. 2:

- single (double, triple, etc.) photoelectron(s) peak(s) is(are) clearly visible;
- one very easily can estimate the SiPM gain, using single photoelectron peak, which obviously corresponds to the single pixel fired: $Gain = Q_{one\ pixel}/e$, where e is the electron charge;
- pixel-to-pixel gain variation is rather small, i.e., the pixel capacitance is quite uniform: $\sigma_1/\mathrm{S}_1 \simeq$ 10%, where S_1 and σ_1, are single pixel signal and its dispersion, respectively;
- SiPM excess noise factor (ENF), responsible for pixel-to-pixel gain variation $ENF = 1+\sigma_1^2/S_1^2$ is very small;
- the contribution of electronics noise (pedestal width) is also very small;
- SiPM gain and photon detection efficiency (compare Figs. 2a and b) are overvoltage ΔV=V$_{bias}$-V$_{breakdown}$ and temperature dependent.

2.3 Sensitivity of the SiPM Gain

Figure 3a shows the SiPM gain vs V_{bias} dependence for different temperatures and light wavelengths. The experimental points in Fig. 3a have been obtained by measuring the single photoelectron peak positions (see Fig. 2). The voltage and temperature sensitivity of the SiPM gain can be obtained from Fig. 3a data and is rather weak compared, for instance, to standard avalanche photodiodes (APD). Indeed, we obtain the following dependencies at V_{bias}=24.5V (gain $\simeq 1.5 \cdot 10^6$):

- Gain variation vs overvoltage $dG/G \simeq 7 \cdot dV_{bias}/V_{bias}$, which gives $dG/G \simeq 3\%$ for dV_{bias}=0.1 V;
- Gain variation vs temperature $dG/G \simeq 1.3 \cdot dT/T(^o\mathrm{K})$, which gives dG/G=0.5% for $dT=1^o$ and T=-20^{o}C.

Such a voltage and temperature variations of the SiPM gain have to be compared with the same values for avalanche photodiodes[3]: $dG/G = 75 \cdot dV/V_{bias}$ and $dG/G = 17 \cdot dT/T$ for an APD gain of 100.

The low voltage and temperature sensitivity of SiPM gain is an important practical advantage compared to the APD.

2.4 SiPM Dynamic Range

The SiPM dynamic range is limited due to the finite total pixel number m at $N_{ph} \cdot \varepsilon/m < 1$, where N_{ph} is the number of photons, and ε - the photon detection efficiency. This means that the average number of photoelectrons per one pixel should be small enough. The finite pixel number m results in the saturation of the SiPM signal with increased light intensity (or the average number of photoelectron per each pixel) (see Fig. 3b). The signal dispersion, in terms of the number of photoelectrons, can be calculated using this curve. Figure 3c shows the deviation of the signal dispersion from Poissonian value $\sigma = \sqrt{N_{phe}} = \sqrt{N_{ph} \cdot \varepsilon}$, as a function of light intensity. As can be seen from Fig. 3c the value of σ is quite close to Poissonian for $N_{phe}/m \leq 0.6$, and dramatically increases for large N_{phe}/m values due to saturation of the SiPM signal.

In conclusion, the SiPM dynamic range is determined by deterioration of the signal dispersion at $N_{phe} \geq 0.6 \cdot m$. The increase of total pixel number m seems technologically possible up to $\sim$4000 mm^{-2}; therefore, the SiPM dynamic range of up to $2.5 \cdot 10^3$ phe/mm^2 is feasible.

2.5 SiPM Photon Detection Efficiency

The SiPM photon detection efficiency is $\varepsilon = QE \cdot \varepsilon_G \cdot A_{pixels}/A_{total}$, where QE is the quantum efficiency (typically 0.5-0.8, wavelength dependent), A_{pixels}/A_{total} is the so-called geometrical efficiency that is a fraction of total the SiPM area, occupied by active pixel area A_{pixel} and ε_G is probability

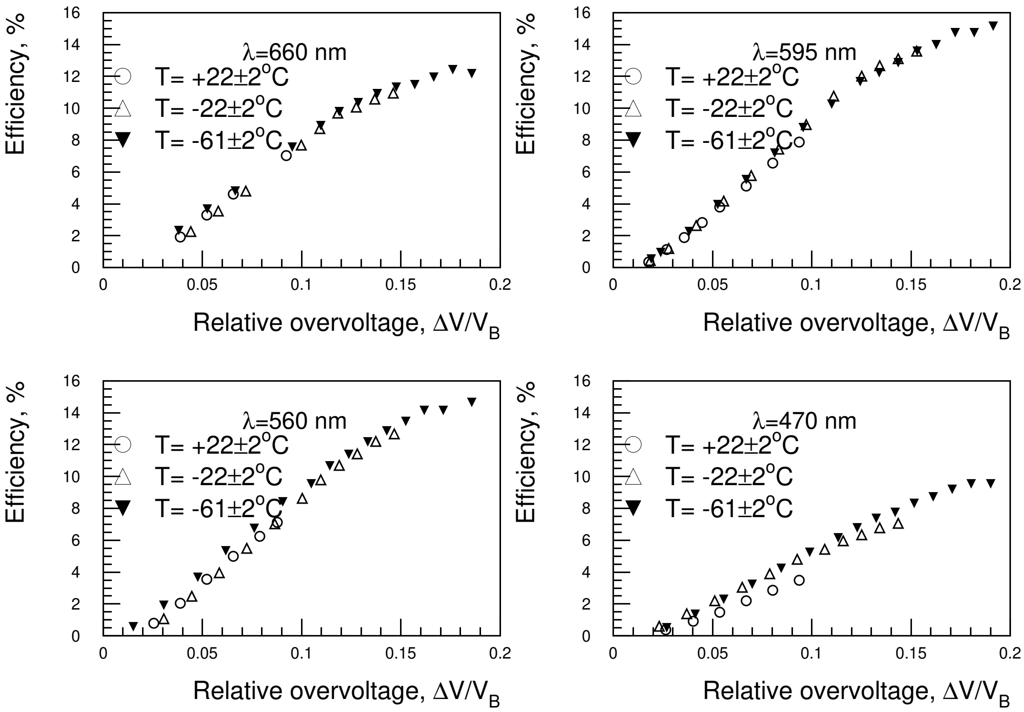

Figure 4: SiPM photon detection efficiency for different temperatures and light wavelengths.

for a carrier created in active pixel area to initiate a Geiger-mode discharge. The photon detection efficiency has been measured using a different wave-length light emission diodes and the calibrated PMT and is shown in Fig. 4 as function of relative overvoltage $OV = (V_{bias} - V_{breakdown})/V_{breakdown}$. One can see, that efficiency for the visible light is comparable to standard vacuum PMT with bialcali photocathode for green and blue light and even better in yellow-red region. The SiPM photon detection efficiency achieved is significantly higher compared to our previous paper[1]. The SiPM performance is limited for $OV >$ 1.15 - 1.20 due to the increase of dark noise rate.

2.6 SiPM Noise

The electronics noise ib SiPMs is negligibly small because of very high gain ($\sim 10^6$), in contrast to standard avalanche photodiodes, where the gain is typically 100-200. Actually, the level of electronics noise is less than 0.1 electrons (see Fig. 2, pedestal width).

The main source of noise limiting the SiPM performance is dark noise rate, which originates from the carriers created thermally in sensitive volume and also due to the effects of high electric fields[4]. The SiPM dark rate decreases with temperature from a few MHz/mm^2 (room temperature) to $\sim$1kHz/mm^2 (at 100^{o}K).

Such a dark noise rate limits SiPM performance at temperatures above 0^{o}C, especially for large sensitive area ($\sim$1 cm^2), and needs to be reduced by improving pixel production technology. However, SiPM's dark noise rate limits SiPM performance only in detection of very small light intensities (one or a few photoelectrons), and it does not affect in the case of larger light signals.

2.7 Timing by SiPM

The development of the Geiger-type discharge, for a very small width of depletion region, is very fast (a few hundred picoseconds). The typical rise time observed is $\sim$1 ns, the decay time is determined by the time constant $C_{pixel} \cdot R_{pixel}$=30 ns, thus, the recovery time of a single SiPM pixel is <100 ns and a much smaller recovery time for the whole SiPM is expected.

Timing with SiPMs has been studied using a very fast red-laser diode (λ=670 nm, light signal width of 40 ps). Figure 5a shows the time resolution (r.m.s.) as a function of the number of pixels fired for photons absorbed in the Geiger region. One observes very good timing resolution, which follows the Poissonian law $1/\sqrt{N_{pixels\ fired}}$. Figure 5b shows a shift of the time distributions for a displacement in space of the laser source. There is a clear separation between the peaks for the displacement of 30 mm with an r.m.s. value of about 7.5 mm.

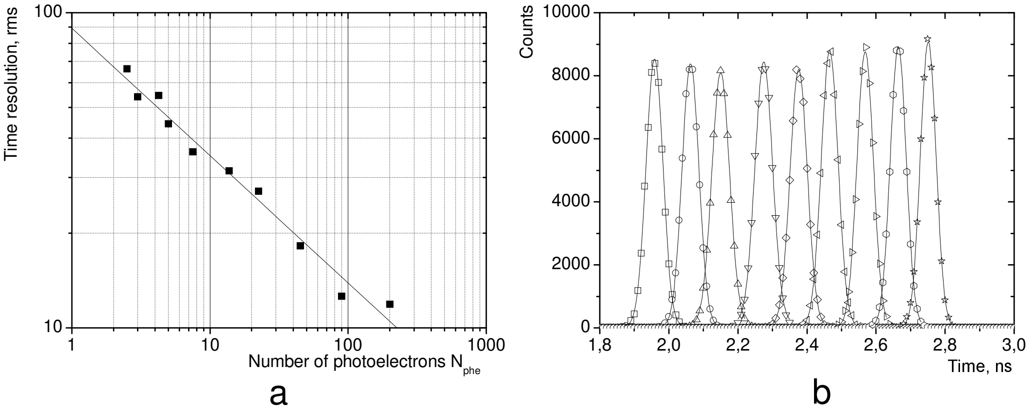

Figure 5: (a) SiPM time resolution and (b) time spectra for different positions of the light source shifted by 30 mm.

3 Experimental Tests for Possible SiPM Applications

3.1 Scintillation Fiber Detector: SiPM vs APD Comparison

The relativistic particle detection by scintillation fiber has been studied using an $Sr^{90}\beta$-source and multicladding Kuraray scintillation fiber SCSF-3HF (1500)M with a core diameter of 0.94 mm, an emission peak of 530 nm, a decay time of 7 ns, and 1/e length of >4.5 m.

The results of the measurements are shown in Fig. 6, together with the results obtained with the the APD on a similar measurement, (a gain of 100-500, and a quantum efficiency QE of 70%)[5]. The SiPM has a much lower photon detection efficiency (15%); however due to: 1) practical absence of electronics noise and 2) a lower ENF factor, the SiPM performs approximately as good as the APD (in terms of signal/noise ratio).

3.2 Plastic Scintillator + Wavelength Shifter (WLS) Readout: SiPM vs APD Comparison

The plastic scintillator with a wavelength shifter (WLS) readout has become a more and more popular device, because of the need to readout a very large number of scintillators (e.g., preshower[6] or tile calorimeters[7]). In addition, due to the small space available and the need to perform in a high magnetic field, the usage of PMT readout is difficult. Therefore, the Si-based photodetectors (like the APD) look more promising.

We have carried out test measurements with a plastic scintillator and a WLS readout* using

*We used the scintillation counter and WLS fiber readout produced by V.Semenov (IHEP).

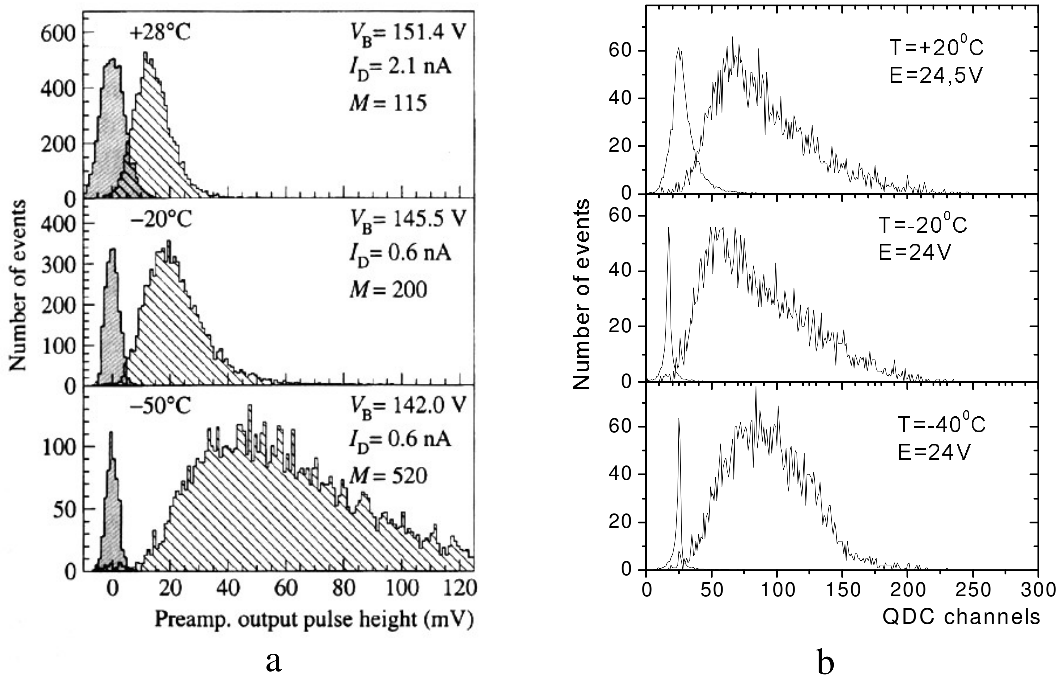

Figure 6: Comparison of (a) APD and (b) SiPM spectra from relativistic particles detected by scintillation fiber.

SiPM. Figure 7 shows the test results for a plastic scintillator, 14x14 cm^2 and 4 mm thickness, for minimum ionizing particles (cosmic muons and electrons from an Sr^{90} source). For optical readout, we used fiber with 1 mm diameter and WLS (λ=494 nm), and a length of 1.5 m. The loop of the WLS fiber was embedded in a plastic body, with one end of the fiber covered by an aluminized mirror in order to increase the light collection, the other one was connected to the SiPM. The results for the SiPM readout are compared in Fig.7 with similar APD results[6], where scintillation light detection was used. We can see that despite the lower SiPM photon detection efficiency, the MIP detection looks favorably to the SiPM (again, due to a much lower electronics noise and ENF value).

3.3 TESLA Hadron Tile Calorimeter Readout Using SiPMs

We have studied the possibility of a tile scintillator and a WLS fiber readout with an Si photomultiplier, for example, for the Tesla Hadron Tile Calorimeter experiment[8].

The calorimeter has a tower-like scintillator tile structure; each tower consists of scintillator cells with a minimum three scintillator tiles in one cell (front side), and a maximum of 7 scintillator tiles in one cell (back side). Each 5-mm thick tile scintillator is readout by a WLS fiber with 1 mm

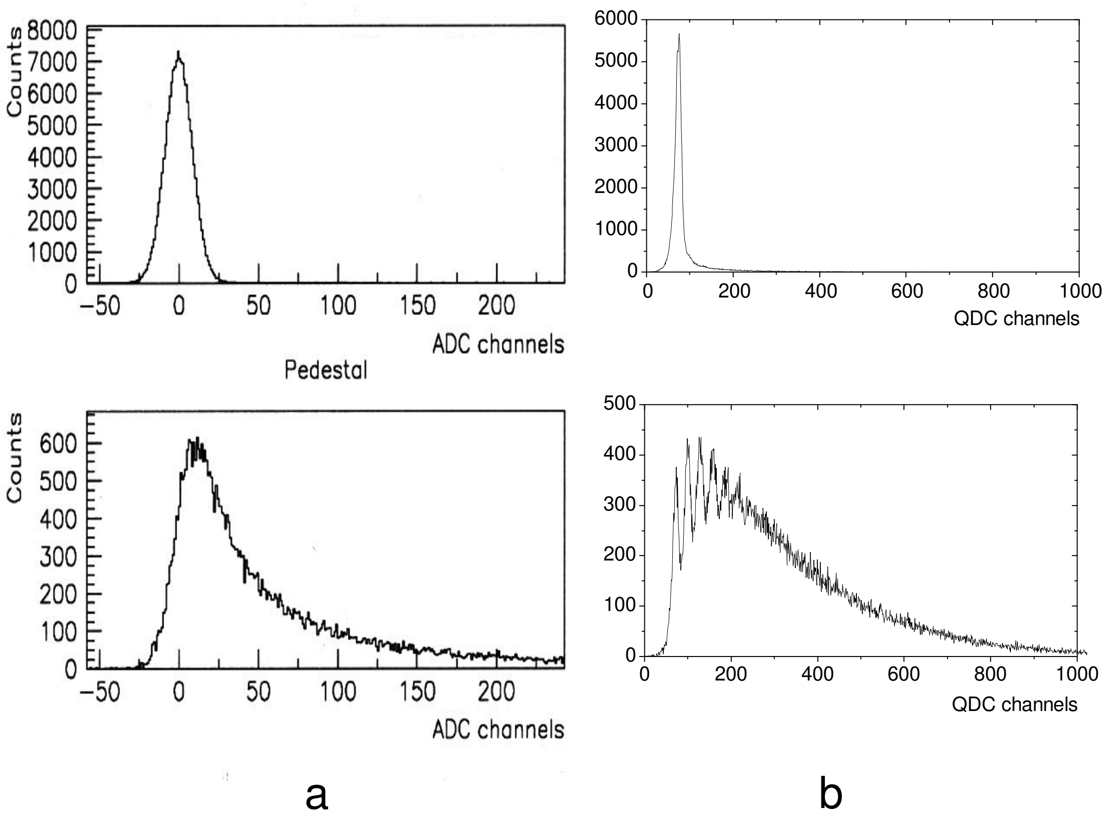

Figure 7: Comparison of APD (a) and SiPM (b) spectra from relativistic particles detected by plastic scintillator + WLS.

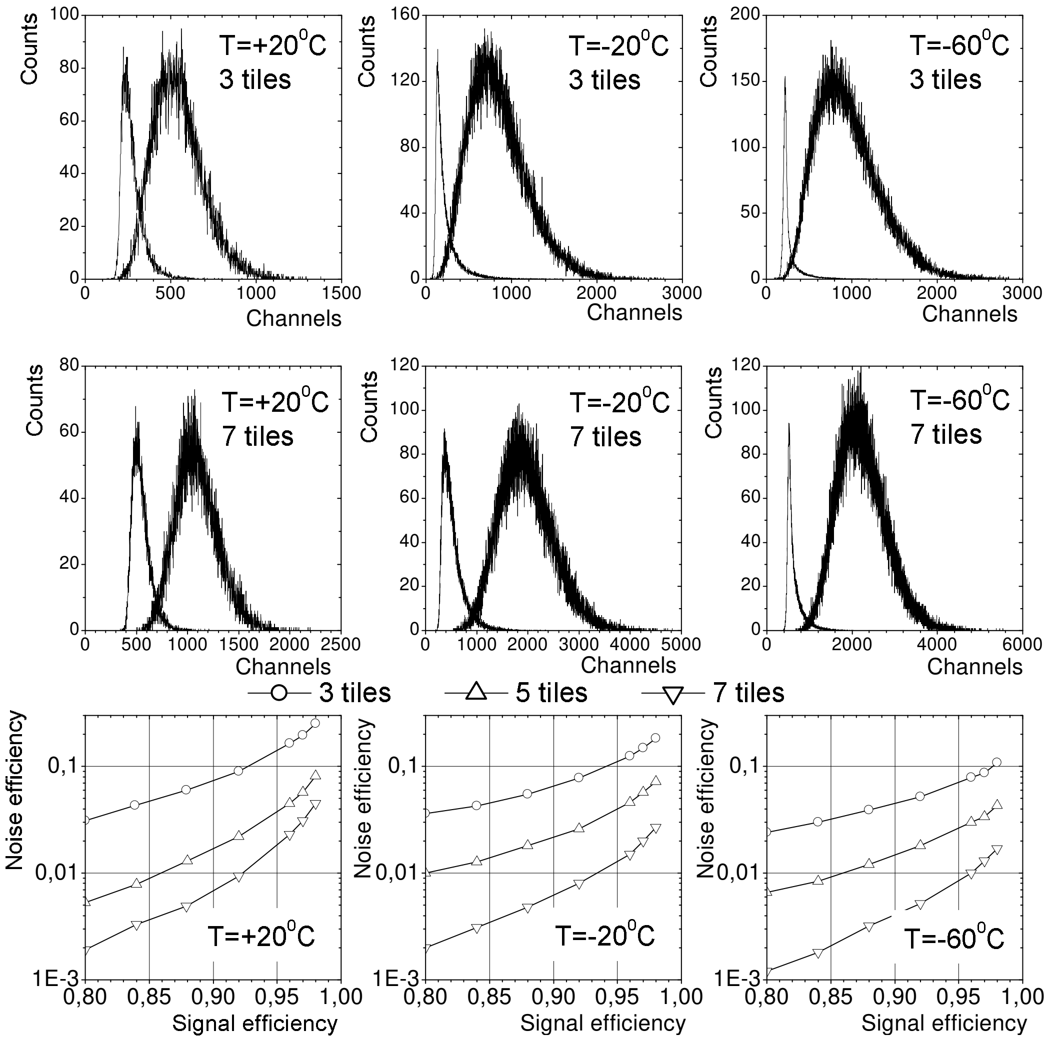

Figure 8: SiPM performance for TESLA HCAL (see text).

in diameter.

The TESLA hadron calorimeter required a dynamic range of photodetectors as determined by[8]:

- minimal signal: MIP (muons, used for calibration purposes), expected number of scintillator photons: n_{min}=60/3tiles=20photons/mm^2 of SiPM;
- maximal signal: high-energy jet, the expected number of photons is n_{max}=3.6·10^4/7tiles $\simeq$ 5·10^3 photons/mm^2 of SiPM.

To decrease the impact of the SiPM signal saturation (see Fig.3b) and meet the $n_{max} \cdot \varepsilon/m < 0.6$ requirement, we need to have the number of SiPM pixels per 1mm^2 $m \geq 5{\cdot}10^3{\cdot}0.15/0.6 \simeq 1200$ for photon detection efficiency of ε_{ph}=0.15. The SiPM is undergoing modifications to increase the number of pixels to 2500 mm^{-2} at "Pulsar" enterprise (Moscow). In order to demonstrate the feasibility of TESLA hadron calorimeter calibration by an MIP, we used the experimental data for one tile and superimposed 3, 5, or 7 tiles together. The results of such a superposition, which simulates the calorimeter cells response with 3 and 7 tiles, are shown in Fig.8. We can see a good MIP signal/noise ratios (shown in bottom half of Fig.8) which looks promising for utilization within the cell structure of the calorimeter.

4 Conclusions

In conclusion a comparison in Table 1 shows the SiPM characteristics and performance of typical present photodetectors, such as vacuum phototubes (PMT), Si avalanche photodiodes (APD), and hybrid photodetectors (HPD).

As can be seen, Si Photomultiplier appears to be good candidate to complement a wide range of photodetectors.

Acknowledgments

The authors would like to thank Prof. R.Klanner for his close attention and invaluable support during the SiPM research and development work.

This work was supported by the International Science and Technology Center, grant ISTC 1275-99.

Table 1:

	PMT	APD	HPD	SiPM
Photon detection efficiency:				
blue	20%	50%	20%	12%
green - yellow	a few %	60-70%	a few %	15%
red	<1%	80%	<1%	15%
Gain	10^6-10^7	100-200	10^3	10^6
High voltage	1-2 kV	100-500 V	20 kV	25 V
Operation in the magnetic field	problematic	OK	OK	OK
Threshold sensitivity S/N$\gg$1	1 ph.e.	$\sim$10 ph.e.	1 ph.e.	1 ph.e.
Timing /10 ph.e.	$\sim$100 ps	a few ns	$\sim$100 ps	30 ps
Dynamic range	$\sim 10^6$	large	large	$\sim 10^3/\mathrm{mm}^2$
Complexity	high (vacuum, HV)	medium (low noise electronics)	very high (hybrid technology, very HV)	relatively low

References

[1] G. Bondarenko et al, NIM A242(2000)187 and references therein.

[2] F. Zappa et al, Opt. Eng. 35(4) (1996)938,
S. Cowa et al, J. Appl. Phys. 35(1996)1956 and references therein.

[3] A. Karar et al., NIM A428(1999)413.

[4] G. Vincent et al, J. Appl. Phys. 50(1979)5984.

[5] T. Okusawa et al., NIM A459(2001)441.

[6] C. Cheshkov et al., NIM A440(2000)38.

[7] HCAL Technical Design Report, CERN/LHCC 97-31, CMS TDR2, 1997.

[8] Tesla Technical Design Report, v.3,4, DESY 2001-011, March 2001.